

A Fluorescent Chemosensor for Zn²⁺ Based on a C₃-Symmetrical and Pre-Organized 2,2',2''-Nitrilotribenzoic Acid Material

Wenguang Wei,^{A,B} Yao Jin,^{A,B} Tao Han,^{A,B} Bin Du,^{A,B,C} Xiujuan Zhi,^{A,B} Chaojun Wei,^{A,B} and Sichun Yuan^{A,B,C}

^ABeijing Key Laboratory of Agricultural Product Detection and Control of Spoilage Organisms and Pesticide Residue, Beijing Laboratory of Food Quality and Safety, Beijing 102206, China.

^BFaculty of Food Science and Engineering, Beijing University of Agriculture, Beijing 102206, China.

^CCorresponding authors. Email: Bindu80@bua.edu.cn; ysc@bua.edu.cn

A C₃-symmetrical 4,4'',4''''-nitrilotris(2'-methyl-[1,1'-biphenyl]-3-carboxylic acid) (**4**) derived from nitrilotriacetic acid (NTA) was found to selectively bind Zinc(II) ions both in DMSO or MeOH. A synergistic effect of the anionic counter ion SO₄²⁻ on the sensing behaviour of **4** to metal ions was clearly observed in DMSO. Interestingly, **4** showed a rapid hypochromatic shift in emission ascribed to the deprotonation and the concomitant formation of a **4**-metal complex upon the addition of Zn²⁺ ions, instead of the bathochromic shift and emission enhancement attributed to the SO₄²⁻-involved hydrogen-bonding interaction for Ni²⁺, Li⁺, Mg²⁺, and Na⁺ ions at ratios below 1:1 in DMSO. The observed sensing process of sulfate salts associated with the SO₄²⁻-involved hydrogen-bonding interaction, deprotonation, and the concomitant complexation can also be clearly monitored by titration methods utilising UV-vis, fluorescence, and NMR spectroscopy in solution. In comparison with **4**, compound **1** showed an obvious difference in the binding interaction with zinc sulfate in MeOH, probably owing to the decreased acidity. Anion-induced hydrogen-bonding interactions and deprotonation of the COOH protons in the excited state also endowed **4** versatile spectroscopic properties. The addition of F⁻ and SO₄²⁻ anions resulted in a remarkable enhancement probably related with a rigidifying effect. 2,2',2''-Nitrilotribenzoic acid can be utilised as a potential scaffold to build a series of conjugated fluorescent sensors by its chelation effect owing to the rigid cavity pre-organised by the triphenylamine moiety and the carboxylic groups and the conjugation extension in the 4,4',4'' positions.

Manuscript received: 5 July 2018.

Manuscript accepted: 8 September 2018.

Published online: 11 October 2018.

Introduction

Over the past decades, acyclic N,O ligands such as iminodiacetic acid (IDA), nitrilotriacetic acid (NTA), bis(2-pyridylmethyl)amine (BPA), tris(2-pyridylmethyl)amine (TPA), tri(2-aminoethyl)amine (TREN), and their derivatives serving as well known heavy metal chelators, have attracted much attention in molecular recognition.^[1-4] Nitrilotriacetic acid has been widely used as a chelate for more than 60 metal ions. Carboxylate donor groups containing a central nitrogen atom can allow tetradentate chelation, leading to the higher stability of the NTA complexes in comparison with the corresponding IDA analogues. In addition, the capability of their corresponding transition metal complexes to selectively bind Lewis basic guest molecules in competing solvents renders them as potential synthetic receptors applicable in chemical biology or biotechnology.^[5-10] In recent years, many other NTA-based fluorescent sensors have been developed by the attachment of the chromophores using the unconjugated chain. However, as NTA analogues, 2,2',2''-nitrilotribenzoic acid derivatives (Chart 1; 2,2',2''-NTBA) haven't been investigated for their potential application in

fluorescent sensors. The carboxylic groups and nitrogen atom directly blended into the conjugation system can probably endow them versatile photophysical properties when they interact with ions, due to interweaving of the π -system and recognition element.^[11-16]

This article reports the synthesis and evaluation of the fluorescent properties of C₃-symmetrical 4,4'',4''''-nitrilotris(2'-methyl-[1,1'-biphenyl]-3-carboxylic acid) (**4**) when interacting with ions in solvent. Triphenylamine (TPA) introduced as the electron donor and the three carboxylic acids used as anion and cation binding sites, can pre-organise to form a rigid cavity. The lone electron pair of the nitrogen atom on the TPA can coordinate metal ions. Compound **4** demonstrated versatile fluorimetric signals when exposed to anion- or cation-containing solutions, due to conformational changes, internal charge transfer (ICT), and the formation of metal complexes attributed to the assistance of hydrogen-bonding interactions, which makes it a promising skeleton for a fluorescent sensor for rapid, simple, and low-cost methods for ion detection.

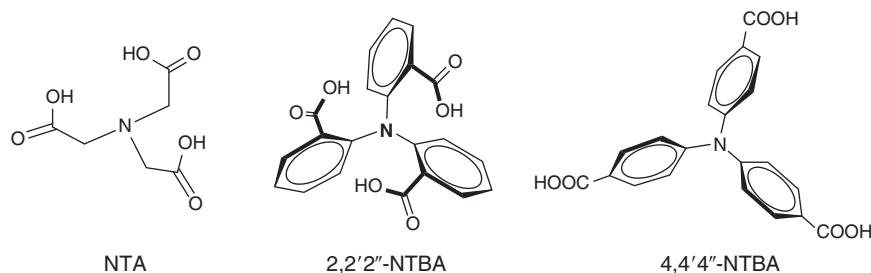


Chart 1. The molecular structure of metal chelators.

Experimental

Materials Synthesis

All chemicals were used as received unless otherwise indicated. All oxygen and moisture sensitive reactions were performed under nitrogen atmosphere. Reagent grade tetrahydrofuran (THF) was distilled over sodium and benzophenone.

Synthesis of the 2,2',2''-Nitrilotribenzoic Acid (**1**)

To a solution of trimethyl 2,2',2''-nitrilotribenzoate (0.42 g, 1.0 mmol) in a mixture of ethanol and water (100 mL), was added potassium hydroxide (3.25 g, 58 mmol) and the solution refluxed overnight. The acid was precipitated by the slow addition of 1 N HCl (aq) to the aqueous phase. The white precipitate was filtered off and thoroughly dissolved in ethyl acetate. The organic layer was washed with deionized water and dried over anhydrous MgSO_4 . After evaporating the solvent, a white powder was obtained (0.34 g, 90%). δ_{H} (300 MHz, methanol- d_4) 7.84 (b, 3H), 7.44–7.41 (t, 3H), 7.23–7.20 (t, 3H), 6.83 (b, 3H). δ_{C} (75 MHz, methanol- d_4) 168.45, 147.91, 132.84, 131.90, 126.53, 125.17, 124.17. m/z (ESI) 376.2 ($[\text{M} - \text{H}]^-$); calcd for $\text{C}_{21}\text{H}_{14}\text{NO}_6$ 376.1.

Synthesis of the Trimethyl 6,6',6'''-Nitrilotris(3-bromobenzoate) (**2**)

N-Bromosuccinimide (1.37 g, 7.89 mmol) was added to a THF solution (40 mL) of trimethyl 2,2',2''-nitrilotribenzoate (1.00 g, 2.39 mmol) and stirred overnight at room temperature. After the addition of deionized water and chloroform, the organic layer was washed with water and sodium chloride. The organic layer was dried over anhydrous MgSO_4 . After evaporating the organic solvent, the residue was purified by column chromatography (petroleum ether/ethyl acetate = 4:1) to afford a pale-yellow product (1.38 g, 89%). δ_{H} (400 MHz, CDCl_3) 7.74–7.73 (d, 3H), 7.48–7.46 (dd, 3H), 6.92–6.89 (d, 3H), 3.45 (s, 9H). δ_{C} (100 MHz, CDCl_3) 165.73, 145.26, 135.34, 133.71, 129.15, 127.51, 116.82, 52.14. Anal. Calc. for $\text{C}_{24}\text{H}_{18}\text{Br}_3\text{NO}_6$: C 43.93, H 2.77, N 2.13. Found: C 43.72, H 2.57, N 2.23 %.

Synthesis of the Trimethyl 4,4',4'''-Nitrilotris(2'-methyl-[1,1'-biphenyl]-3-carboxylate) (**3**)

A mixture of **2** (2.13 g, 3.26 mmol), *o*-tolylboronic acid (2.67 g, 16.3 mmol), NaHCO_3 (3.28 g, 39.10 mmol), $\text{Pd}(\text{PPh}_3)_4$ (0.19 g, 0.163 mmol) in THF (15 mL), and deionized water (20 mL) were refluxed overnight under nitrogen atmosphere. The mixture was extracted with ethyl acetate. The organic extract was dried over MgSO_4 . After removal of solvents under reduced pressure, the residue was purified by column chromatography (petroleum ether/ethyl acetate = 100:8) to afford **3** as a pale-yellow solid (2.03 g, 70%). δ_{H} (400 MHz, CDCl_3) 7.61–7.60

(d, 3H), 7.41–7.38 (dd, 3H), 7.27–7.22 (m, 15H), 3.47 (s, 9H), 2.32 (s, 9H). δ_{C} (100 MHz, CDCl_3) 167.56, 145.70, 140.35, 137.27, 135.32, 133.02, 131.67, 130.47, 129.69, 127.57, 127.16, 125.93, 125.85, 51.76, 20.53. m/z (ESI) 690.3 ($[\text{M} - \text{H}]^-$); calcd for $\text{C}_{45}\text{H}_{40}\text{NO}_6$ 690.2.

Synthesis of the 4,4',4'''-Nitrilotris(2'-methyl-[1,1'-biphenyl]-3-carboxylic acid) (**4**)

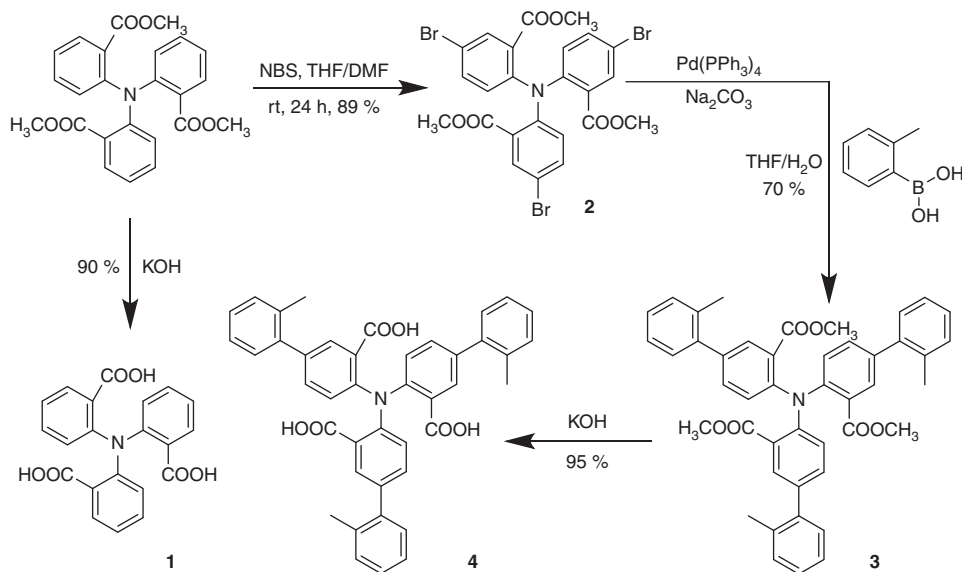
To a solution of compound **3** (2.00 g, 2.90 mmol) in a mixture of ethanol and water (150 mL) was added potassium hydroxide (32.50 g, 580 mmol) and the solution refluxed overnight. The reaction was terminated when the starting material was fully consumed, which was detected by column chromatograph. The acid was precipitated by the slow addition of 1 N HCl (aq) to the aqueous phase. The white precipitate was filtered off and thoroughly dissolved in ethyl acetate. The organic layer was washed with deionized water and NaCl and dried over anhydrous MgSO_4 . After evaporating the solvent, a pale-yellow powder was obtained (1.80 g, 95%). δ_{H} (400 MHz, d_6 -DMSO) 12.75 (b, 3H), 7.71 (b, 3H), 7.53–7.51 (b, 3H), 7.33–7.26 (m, 12H), 6.98 (b, 3H), 2.28 (s, 9H). δ_{C} (100 MHz, d_6 -DMSO) 167.24, 146.07, 139.66, 136.98, 134.79, 133.44, 131.98, 130.49, 129.32, 127.59, 126.51, 126.10, 124.88, 20.15. m/z (HRMS ESI) 646.2232; calcd for $\text{C}_{42}\text{H}_{32}\text{NO}_6$ $[\text{M} - \text{H}]^-$ 646.2235.

Characterisation and Instruments

NMR spectra were obtained on a Bruker (300 or 400 MHz) using CDCl_3 , methanol- d_4 , or $\text{DMSO}-d_6$ as the solvent unless otherwise noted. High resolution mass spectrometry (HRMS) experiments were performed on an FT-ICR-MS spectrometer (APEX II). The crystal data of compound **1** was collected using a Bruker APEX II. Acetonitrile (HPLC reagent), THF (HPLC reagent), DMSO (HPLC reagent), and methanol (HPLC reagent) were purchased from Acros Reagent Corporation and used as received. Sodium salts of F^- , Cl^- , Br^- , I^- , NO_3^- , SO_3^{2-} , SO_4^{2-} , AcO^- , S^{2-} , and all metal sulfates were purchased from Xiya Reagent Corporation and dissolved in deionized water. UV-Vis spectra were determined on a Varian Cary 50 UV-vis spectrophotometer at room temperature. For a typical titration experiment, an aqueous solution of metal salt was added to a 5 mL solution of **4** using a pipette. Emission spectra were measured on a Varian Cary Eclipse spectrofluorophotometer at room temperature. All data were manipulated by using the *OriginLab* software package.

General Spectroscopic Methods and Theoretical Calculations

To determine the stoichiometry of metal complexation, the Job's plot method was performed by keeping the total concentration of **4** and the metal ions constant and by changing the mole



Scheme 1. The synthetic route of compound 1–4.

fraction of metal ions from 0 to 1. The mole fraction of metal ions at which the maximum absorption or emission intensity was observed in the plot indicated the stoichiometry of the complex. The binding constant of the compound **4**–Zn²⁺ interaction was evaluated from the absorbance measurement and obtained using the Benesi–Hildebrand equation.^[13] The geometry was optimized by density functional theory (DFT) calculations using the B3LYP hybrid functional with a basis set limited to 6–31G(d). The molecular orbital shapes and energies were those calculated at optimized geometries with 6–311+g(d, p). Quantum chemical calculations were performed with the *Gaussian03* package and orbital pictures were prepared using *Gaussview*.^[17]

Results and Discussion

Synthesis and Characterization

The synthetic approach to compounds **1–4** are shown in Scheme 1. Subsequent bromination of trimethyl 2,2',2''-nitrilotri(3-bromobenzoate) afforded trimethyl 6,6',6''-nitrilotris(3-bromobenzoate) (**2**) in the presence of NBS with 89% yield. The Suzuki coupling reaction between **2** and *o*-tolylboronic acid was employed to produce trimethyl 4,4',4''-nitrilotris(2'-methyl-[1,1'-biphenyl]-3-carboxylate) (**3**) in 70% yield. Compound **3** underwent a NaOH-promoted hydrolysis to form 4,4',4''-nitrilotris(2'-methyl-[1,1'-biphenyl]-3-carboxylic acid) (**4**) in 95% yield. Compound **1** was synthesized according to the same procedure to produce compound **4**. All new compounds were characterized by ¹H and ¹³C NMR spectroscopy and mass spectrometry.

Unlike 4,4',4''-NTBA in Chart 1,^[18] which has attracted much attention because of its three-dimensional coordination between metal ions and carboxy groups, compound **1**^[19,20] can be pre-organised to form a rigid cavity with three carboxy groups orientated in the same direction, which was confirmed by its single crystal structure (Fig. 1). Thus, we assumed that the 2,2',2''-nitrilotribenzoic acid derivatives have a multifunctionality: (i) the carboxy groups may donate 3-fold hydrogen bonding to an anion and the hydrogen-bonding interaction may increase their acidity; (ii) the pre-organised and tripodal cavity can probably provide a good environment to capture their target ions; (iii) they can be utilised as a potential scaffold to

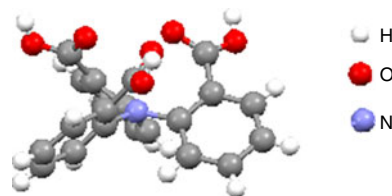


Fig. 1. The single X-ray crystal structure of compound **1**.

build a series of conjugated fluorescent sensors by conjugation extension in the 4,4',4'' positions. In addition, the fluorescent properties of compound **1** and **4** can probably be affected by their conjugation length when interacting with ions in a solvent, owing to their different acidities.

The Binding Behaviours of **4** Towards Ions

Absorption and emission spectroscopic studies of **4** (3.5×10^{-5} M, Fig. 2) have been carried out in a series of protic and aprotic solvents such as THF, DMSO, CH₃CN, and MeOH. Compound **4** showed a broad absorption band centred at 329 nm and a smaller shoulder at 301 nm in DMSO. Absorption spectra of **4** recorded in THF, CH₃CN, and MeOH displayed a 2 nm blue-shift, in comparison with the maxima in DMSO. The shoulder was attributed to the π – π^* transitions, whereas the former was assigned to the ICT transition between the triphenylamine and carboxylic acids. Upon excitation at 325 nm, an emission maxima was exhibited at 464 nm in THF, which red-shifted to 474 nm in DMSO, and further shifted to 495 nm in MeOH. When the polarity of the solvent increased, this solvatochromic red-shift in emission suggested an excited state of **4** with stronger polarity than that in the ground state, and also implied that such absorption bands originated from π – π^* transitions and ICT transitions,^[17] which can be further confirmed by theoretical calculations (Fig. 3). The electron clouds of the highest occupied frontier molecular orbital (HOMO) were mainly localised over the TPA unit, whereas the lowest unoccupied molecular orbital (LUMO) was partially localised in the carboxylic acid moiety, implying compound **4** as a D– π –A molecule. Compound **4** can be pre-organised into a rigid cavity with

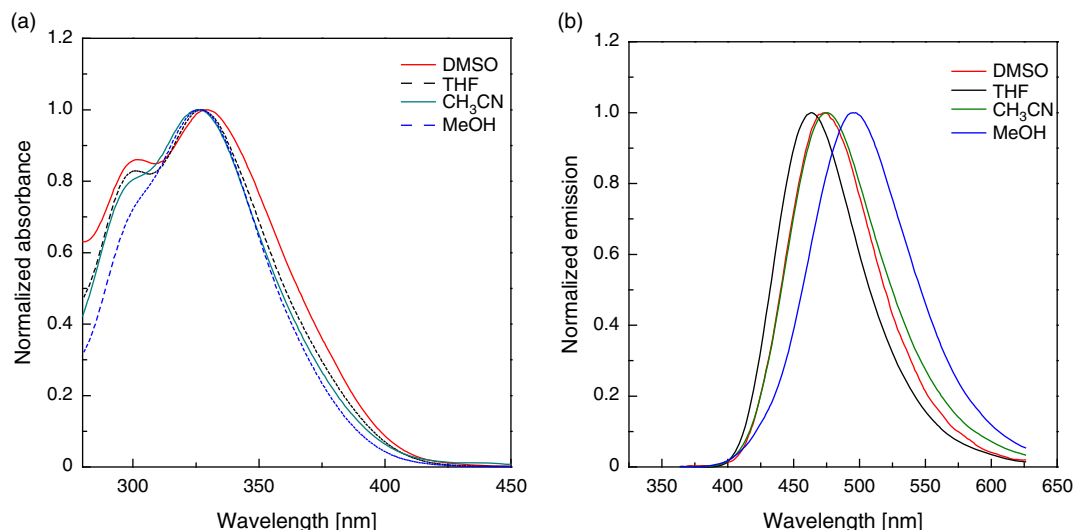


Fig. 2. Absorption and emission spectrum (λ_{ex} 325 nm) of **4** in different solvents.

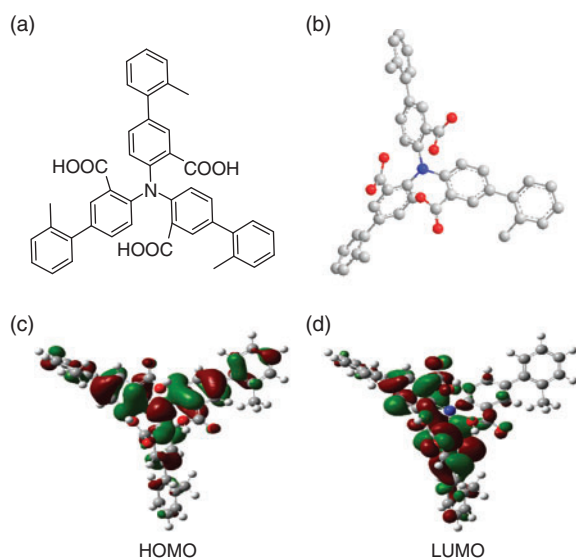


Fig. 3. The structure of **4** (a), optimized molecular structure (b), and orbital plots of HOMO and LUMO energy levels (c and d).

three carboxy groups orientated in the same direction, which was also confirmed by its optimized structure from theoretical calculations.

To explore the ionic sensing behaviours of **4** to metal ions, absorption and fluorescence responses of **4** to different sulfate salts were examined in solution. In the cases of Zn^{2+} , Mg^{2+} , Mn^{2+} , and Li^+ ions, the complex formation respectively induced a hypsochromic shift ($\Delta\lambda$ value) of 25, 32, 20, and 18 nm in DMSO (Fig. 4). The emission peak at 474 nm was markedly blue-shifted to 413, 420, and 421 nm upon addition of the Zn^{2+} , Mg^{2+} , and Li^+ ions, respectively, with a concomitant fluorescence enhancement at the excitation wavelength of 325 nm. The obvious blue-shift in absorption and emission can be attributed to the interaction between the metal cation and the heteroatom of the electron-donating part of the chromophore on the basis of the ICT mechanism widely exploited for cation sensing.^[21] However, upon addition of the same amount of Ni^{2+} , Fe^{2+} , Mn^{2+} , and Cu^{2+} ions, the fluorescence intensity at

474 nm was completely quenched, which is likely ascribed to a strong interaction between transition metal ions and the fluorophore.^[22] Interestingly, Mg^{2+} ions (as their chlorate or nitrate salt) had a negligible effect on the fluorescence and absorption in DMSO solvent, implying the existence of a synergy effect of anionic counter ions on the sensing behaviour of **4** to metal ions (Fig. S1, Supplementary Material). In addition, upon addition of Zn^{2+} ions, the complex formation induced an obvious hypsochromic shift of the long-wavelength absorption band, in a 4×10^{-5} M protic solution (MeOH) of **4** (Fig. 4c). The emission peak at 495 nm was markedly blue-shifted to 445 nm upon addition of Zn^{2+} . It is noteworthy that there were no obvious changes in the absorbance responses of **4** to Mg^{2+} , Mn^{2+} , and Li^+ ions, in comparison with their obvious change of absorption in DMSO. Upon addition of the same amount of Ni^{2+} ions, the fluorescence intensity was moderately quenched with the enhancement of the absorbance band at 300 nm, which was different in comparison with those in DMSO solvent. The absorption peak at 327 nm was acutely blue-shifted after the addition of copper sulfate, which is similar to the capture of Ni^{2+} by **4** in DMSO. Metal ion (as sulfate salts) binding studies of **4** in THF solvent showed behaviours different to those observed in DMSO and MeOH (Fig. S2, Supplementary Material). Among the investigated metal ions, the same amount of sulfate salts induced a negligible change in fluorescence and absorbance, suggesting that the polarity of the solvent played a major role in the metal ion interaction of the receptor. More interestingly, the same amount of sodium and ammonium sulfate salts uniquely induced an enhancement and red-shift in fluorescence and absorbance. The observed spectroscopic changes of **4** in the presence of metal sulfate possibly originated from SO_4^{2-} -involved hydrogen-bonding interactions or a simple deprotonation reaction. SO_4^{2-} possibly increased the receptor's affinity towards ionic guests because the hydrogen bonding can lead to a higher acidity of the benzoic acid group in the excited state, with the formation of contact and/or solvent-separated ion pairs in polar solvents.^[23]

To further gauge selectivity for cations, we also examined metal-coexisting systems in solution. By monitoring the emission peak, Zn^{2+} ions could be distinguished in multimetallic solutions. After the respective addition of Mg^{2+} , Cu^{2+} , Li^+ ,

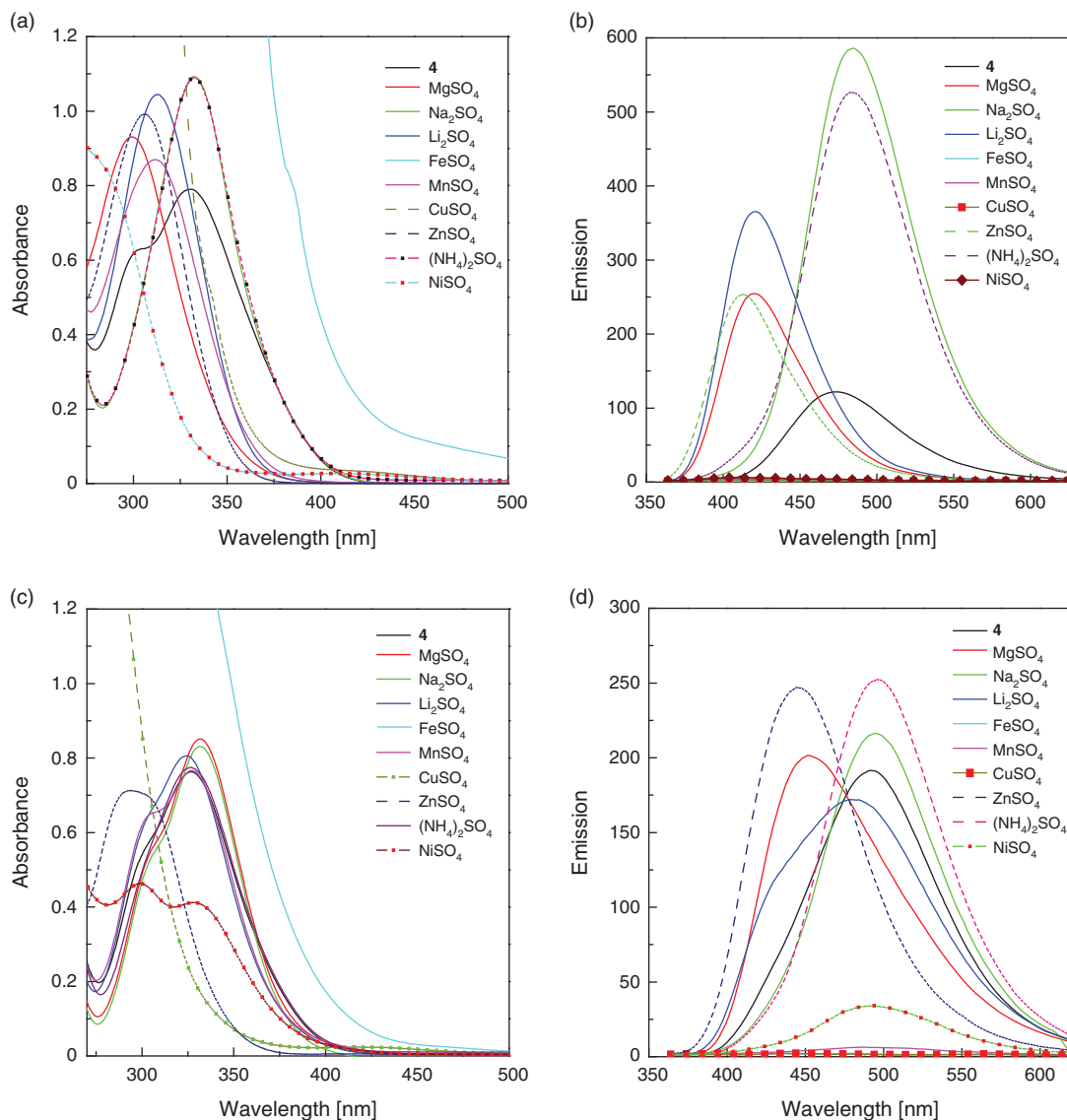


Fig. 4. Absorption and emission spectrum (λ_{ex} 325 nm) of **4** in DMSO (3.5×10^{-5} M, a and b) and MeOH (4×10^{-5} M, c and d) after addition of metal sulfate with the ratio of [metal]/[**4**] (30 : 1).

Ni^{2+} , Fe^{2+} , Mn^{2+} , NH_4^+ , and Na^+ into a solution of **4** in the presence of Zn^{2+} , a close similarity of emission spectrum with those containing only Zn^{2+} was observed in DMSO and MeOH, except for a slight quenching in the cases of Cu^{2+} and Fe^{2+} (Fig. 5 and Fig. S3, Supplementary Material). In MeOH, the emission peaks almost located at ~ 445 nm, which were assigned to the emission of the **4**–Zn complex. The fluorescence emission spectra of **4** in the presence of various cations (Zn^{2+} , Mg^{2+} , Cu^{2+} , Li^+ , Ni^{2+} , Fe^{2+} , Mn^{2+} , NH_4^+ , and Na^+ , as their sulfate salts) in MeOH and DMSO also showed a close resemblance of the emission of those of **4** containing only ZnSO_4 salt (Fig. 6). The results imply that **4** has a high selectivity for Zn^{2+} in the presence of other competitive metal ions. The binding constant of **4**– Zn^{2+} was evaluated as $3.4 \times 10^4 \text{ M}^{-1}$ from the absorbance measurement in MeOH (Fig. S4, Supplementary Material) using the Benesi–Hildebrand equation, and the detection limit of **4** to Zn^{2+} was calculated to be $3.01 \times 10^{-6} \text{ M}$, according to a previously reported procedure.^[13] Although many fluorescent sensors for the detection of Zn^{2+} and Cd^{2+} have been reported, most of them have so far suffered from poor

selectivity.^[2] To further gauge selectivity in distinguishing Zn^{2+} and Cd^{2+} , we conducted competitive experiments by adding Zn^{2+} into the MeOH solution of **4** with Cd^{2+} and adding Cd^{2+} into the solution of **4** containing Zn^{2+} . As shown in Fig. S5 (Supplementary Material), the absorbance and emission spectrum of **4** in the presence of both Zn^{2+} and Cd^{2+} showed a close resemblance to those of **4** containing only ZnSO_4 salt, indicating that **4** can detect Zn^{2+} in the presence of Cd^{2+} .

The Proposed Binding Mechanism

To investigate the synergic effect of SO_4^{2-} on the spectra of **4** in more detail, we performed a titration in DMSO by adding Li^+ , Ni^{2+} , Na^+ , and Mg^{2+} ions. The titration of Li^+ into **4** gave a red-shifted emission centred at 486 nm when the ratio of [salt]/[COOH] is equal to 2 : 1, with a 4.5-fold enhancement of fluorescence. When the ratio exceeded 2.25 : 1, however, the intensity gradually decreased in emission, with the concomitant appearance of a new band centred at 421 nm and a clear isosbestic point at 447 nm (Fig. 7). On the other hand, the absorption of **4** varied remarkably from a 2 : 1 to 4 : 1 ratio, with the

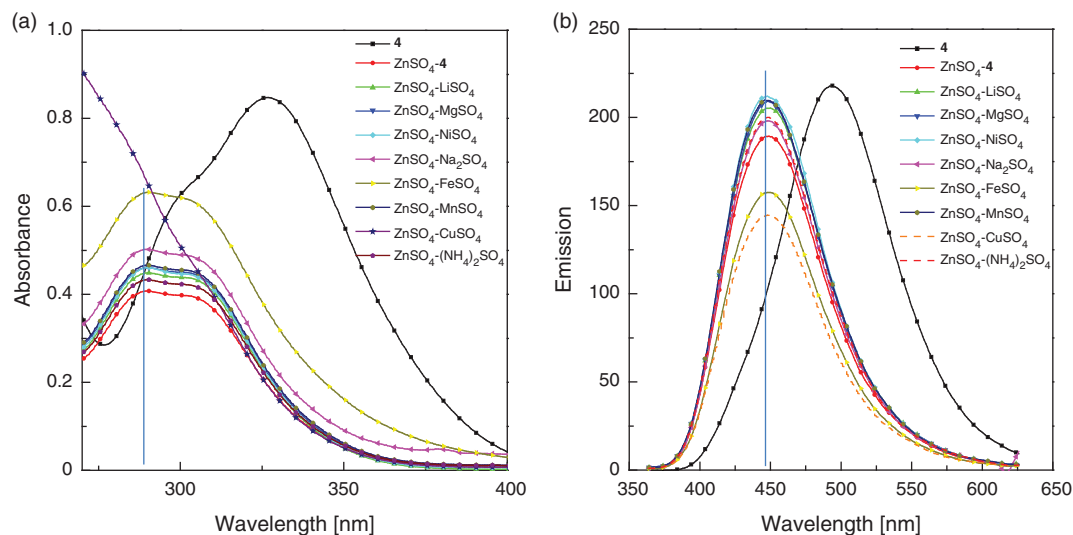


Fig. 5. Absorbance and fluorescence spectrum of **4** (in MeOH, 4×10^{-5} M, λ_{ex} 325 nm), **4** containing 12 equiv. of ZnSO_4 and the spectrum change of **4** containing 12 equiv. of other metal ions with subsequent addition of 12 equiv. of ZnSO_4 .

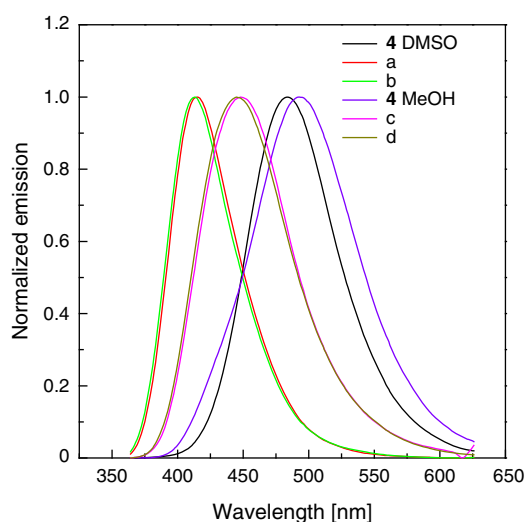


Fig. 6. Normalized fluorescence of **4** (DMSO, 3.5×10^{-5} M and MeOH, 4×10^{-5} M, λ_{ex} 325 nm) exposed to 12 equiv. of various metal ions. (a, c) Normalized emission of **4** containing mixed ions (mix = $\text{Zn}^{2+} + \text{Mg}^{2+} + \text{Cu}^{2+} + \text{Li}^{+} + \text{Ni}^{2+} + \text{Fe}^{2+} + \text{Mn}^{2+} + \text{NH}_4^{+} + \text{Na}^{+}$) in DMSO and MeOH, respectively. (b, d) Normalized emission of **4** containing only Zn^{2+} in DMSO and MeOH, respectively.

concomitant appearance of a new blue-shifted band centred at 313 nm and a clear isoabsorbance point at 321 nm. A Job plot analysis showed that the maximum intensity of fluorescence peaked at 486 nm and appeared at a mole fraction of 0.5, which corresponded to a 1 : 1 ratio ($[\text{Li}_2\text{SO}_4]/[\mathbf{4}]$), under the condition of an invariant total concentration (Fig. 8b). When the ratio exceeded 1 : 1, the intensity gradually increased in emission centred at 421 nm and reached a maximum at $\sim 3 : 1$. Likewise, the absorption peak was red-shifted to a maximum for a 1 : 1 ratio and then blue-shifted to 313 nm for a 3 : 1 ratio (Fig. 8a). Again, the Job plot analysis of Mg^{2+} also showed that the maximum intensity of fluorescence peaked at 486 nm and appeared at a mole fraction of 0.5, and the emission intensity attributed to the metal complexes reached a maximum at a 3 : 1

ratio (Fig. S6, Supplementary Material). The fluorescence titration with Ni^{2+} was recorded in a DMSO solution (Fig. S7, Supplementary Material). When Ni^{2+} was added to the solution of **4**, the fluorescence intensity peaked at 486 nm and was found to be highest at a $\sim 1 : 1$ mole ratio. As the Ni^{2+} content increased beyond the ratio of 1 : 1, the fluorescence gradually decreased and completely quenched at a $\sim 3 : 1$ ratio. From the above description, Li^{+} , Ni^{2+} , and Mg^{2+} sulfate induced the most significant absorbance and emission spectroscopic changes when interacting with **4** in DMSO. Upon the addition of 1 equiv. of metal sulfate, the emission intensity was markedly enhanced with a slight bathochromic shift. Upon further addition of the metal sulfate, the emission was obviously blue-shifted for Li^{+} and Mg^{2+} sulfate, and quenched for Ni^{2+} sulfate. The two-stage absorbance and emission spectroscopic changes signified the presence of two distinctly different equilibrium processes. The enhancement of molecular rigidity and change of electron density ascribed to SO_4^{2-} -involved hydrogen-bonding interactions led to the increase of fluorescent intensity and a spectroscopic red-shift in the first stage with a mole ratio below 1 : 1. In the second stage, a successive blue-shift in emission and absorption were attributed to deprotonation and the concomitant formation of a **4**/metal complex, which will lead to the change in molecular conformation and ICT interaction (Scheme 2).

More interestingly, for the emission spectrum of **4** upon the addition of Zn^{2+} in DMSO (Fig. S8, Supplementary Material), the increase of fluorescence intensity and spectroscopic red-shift, which was attributed to SO_4^{2-} -involved hydrogen-bonding interactions in the early stage, was not observed, instead a rapid deprotonation and complexation was seen, implying the stronger ability of **4** to complex Zn^{2+} over Li^{+} , Ni^{2+} , and Mg^{2+} ions. The titration of **4** with ZnSO_4 salt was also monitored via changes in the ^1H NMR spectrum in d_6 -DMSO. The ^1H NMR spectrum showed proton signals (H_a , H_b and H_c) of **4** at 7.71, 7.55, and 6.98 ppm. With the addition of ZnSO_4 salt, the proton signals (H_a , H_b and H_c) shifted upfield gradually, as shown in Fig. 9. At 1 equiv. of Zn^{2+} , the H_b and H_c signals were split into two, two of them shifted upfield to 7.31 and 6.67 ppm, and the rest remained at the same position. At 3 equiv., the H_a , H_b , and H_c signals completely shifted upfield to 7.69, 7.31, and

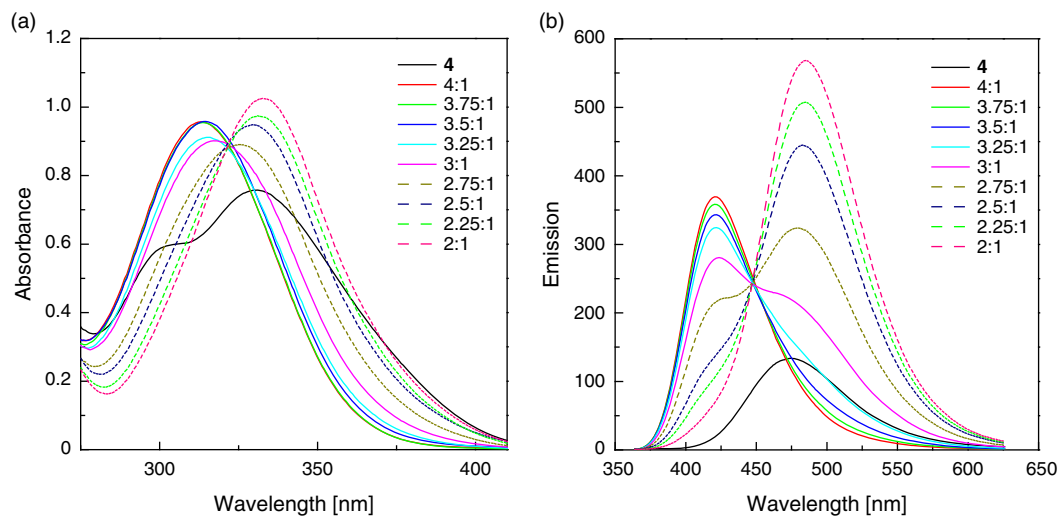


Fig. 7. Absorption and emission spectrum of **4** (3.5×10^{-5} M, λ_{ex} 325 nm) in DMSO after addition of lithium sulfate with the different ratios of [salt] to [COOH]

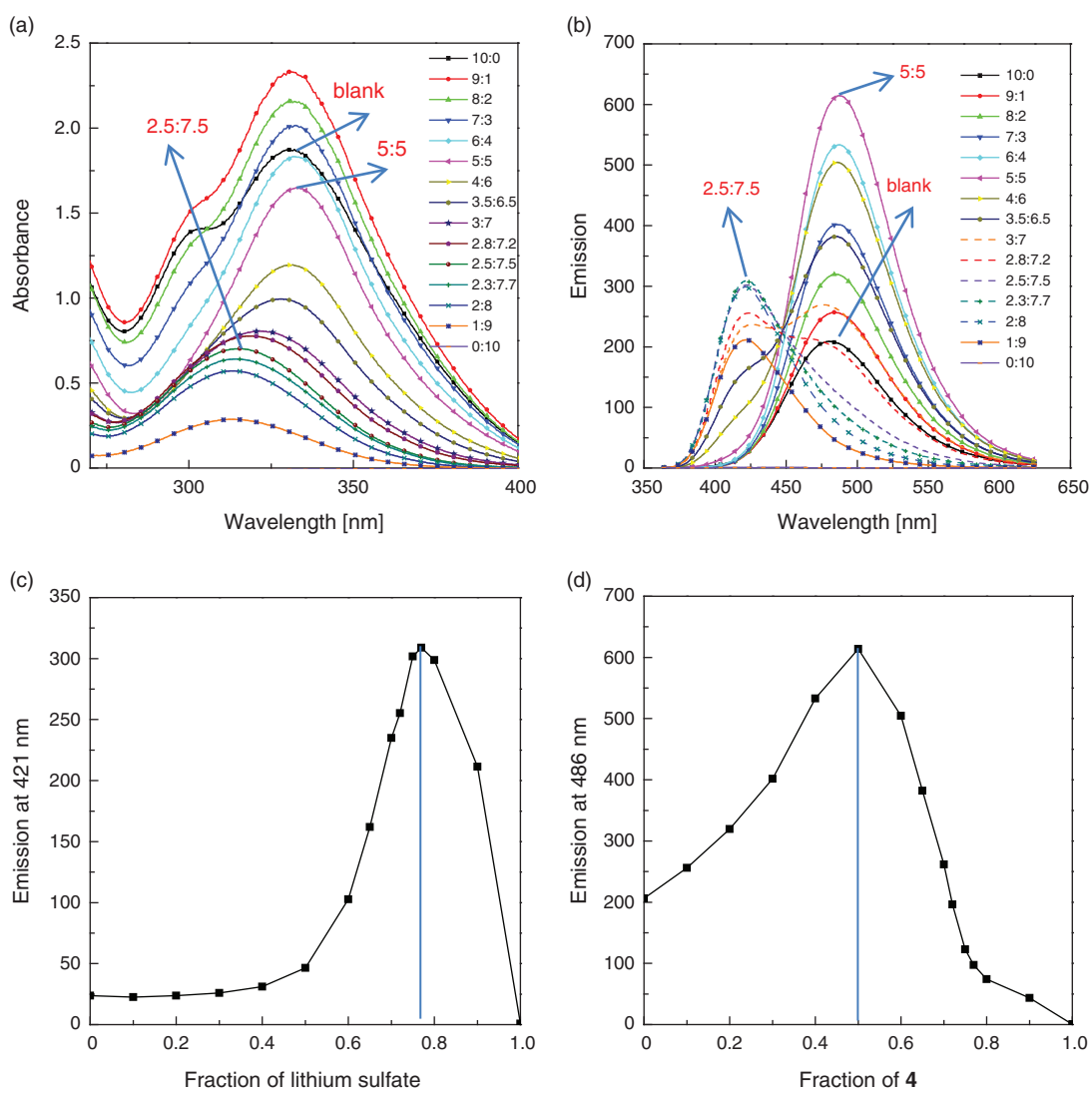
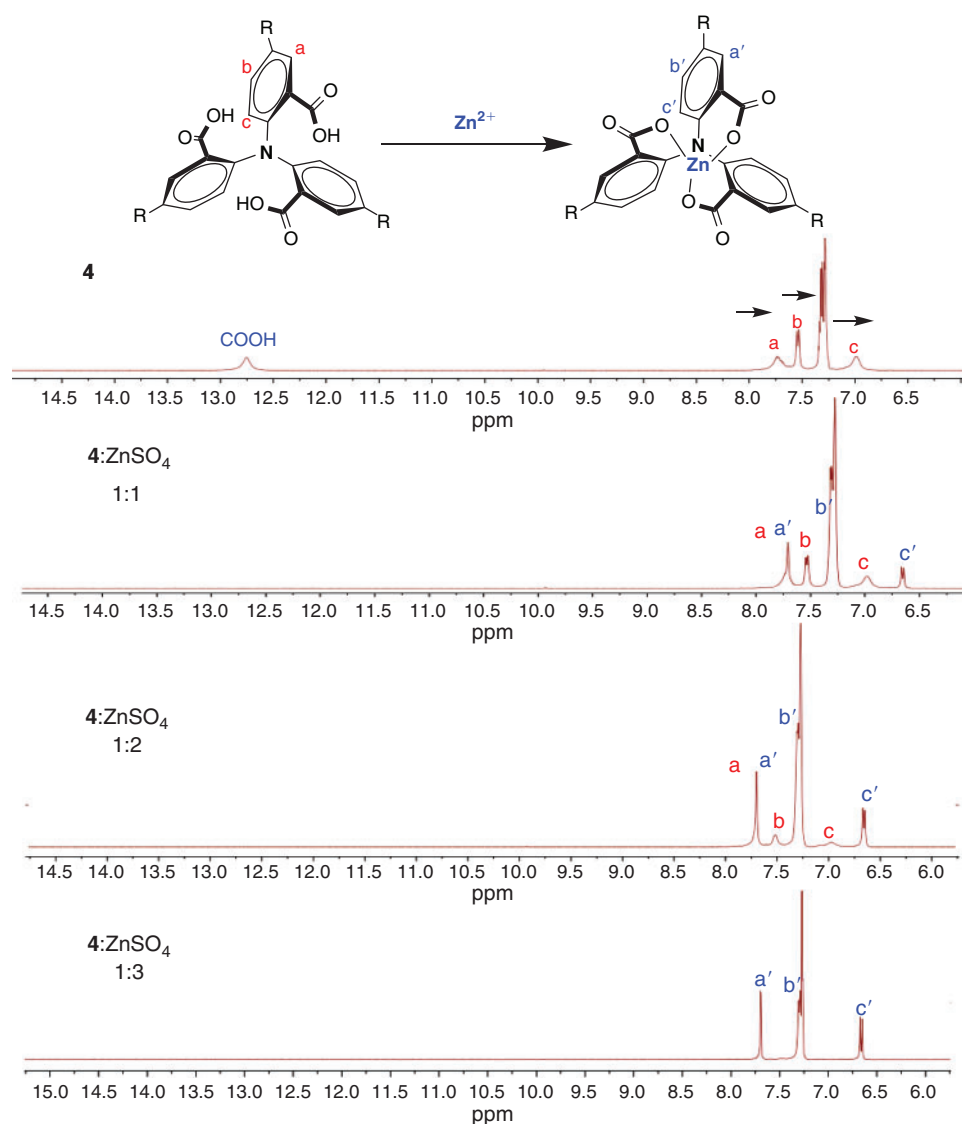
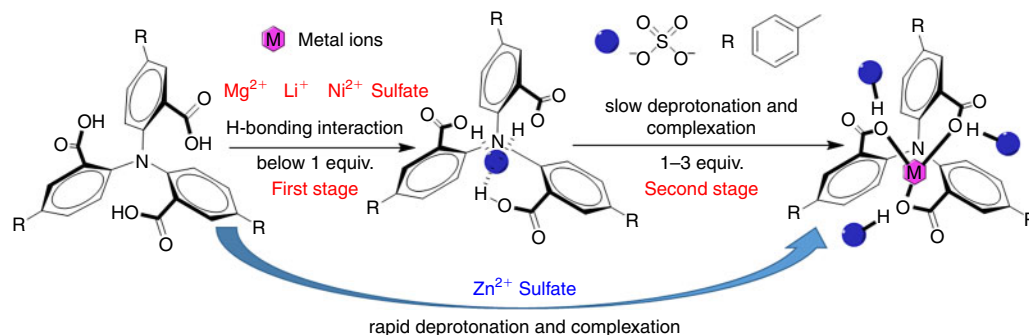


Fig. 8. Absorption and emission spectrum (a and b, λ_{ex} 325 nm) of **4** in DMSO after addition of lithium sulfate with different ratios of [salt] to [**4**], under the conditions of an invariant total concentration (5×10^{-5} M). A Job plot analysis (c and d) between **4** and lithium sulfate.



6.67 ppm. The NMR and spectrophotometric titration clearly showed that compound **4** can show rapid deprotonation and complexation at a low ZnSO_4 concentration below a 1 : 1 ratio. In comparison with the presence of two distinctly different equilibrium processes with Li^+ , Ni^{2+} , and Mg^{2+} sulfate, the rapid deprotonation and complexation was probably the reason

for the high selectivity for Zn^{2+} in the mixed-metal systems. In addition, the binding interaction of compound **1** to Zn^{2+} was also investigated in DMSO, and the emission intensity attributed to the Zn complexes reached its maximum at a 3 : 1 ratio (Fig. S9, Supplementary Material) in the Job plot analysis, which is the same as the 3 : 1 ratio of compound **4**.

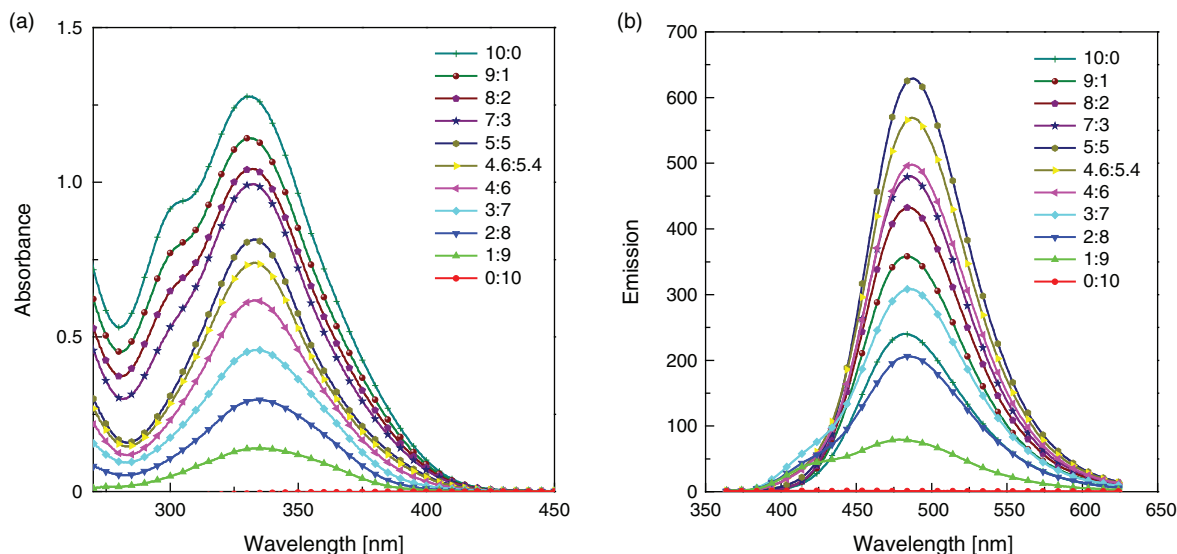


Fig. 10. Absorption and emission spectra of **4** in DMSO after addition of sodium sulfate with different ratios of [salt]/[**4**], under the conditions of an invariant total concentration (5×10^{-5} M, λ_{ex} 325 nm).

The titration of Na^+ into **4** gave a red-shifted emission centred at 486 nm which showed a 6-fold enhancement when the ratio of $[\text{SO}_4^{2-}]$ to $[\text{COOH}]$ was equal to 1.67 : 1 (Fig. S10, Supplementary Material). When the ratio exceeded 1 : 1.25, the emission intensity gradually increased at 486 nm. The absorption of **4** varied remarkably from a 1 : 1 to 1.67 : 1 ratio, with the concomitant appearance of a clear isoabsorbance point at 310 nm. The Job plot analysis of Na^+ showed that the maximum intensity of fluorescence peaked at 486 nm and appeared at a mole fraction of 0.5. When the ratio exceeded 1 : 1, the remarkable emission at 421 nm was not observed, in comparison with the Li^+ and Mg^{2+} ions, which was possibly attributed to the different ability of **4** to capture metal cations under the existence of SO_4^{2-} -involved hydrogen-bonding interactions in the excited state. The absorption peak red-shifted to its maximum at 331 nm at a mole fraction of 0.5 (Fig. 10). With the addition of Na_2SO_4 , the proton signals (H_a , H_b , and H_c ; Fig. S11, Supplementary Material) slightly shifted upfield. At 3 equiv., the H_a and H_b shifted respectively from 7.71 and 7.55 to 7.63 and 7.48 ppm and the H_c remained at the same position. The results are probably due to the increase of electronegativity caused by the hydrogen-bonding interaction between SO_4^{2-} and the carboxy units. In addition, the results also evidence the weak ability of **4** to capture Na^+ to form a chelate. Electrospray ionization mass spectrometry was also utilised to detect labile supramolecules in solution. Mass experiments were performed by adding 30 equiv. of metal sulfate (Mg^{2+} , Cu^{2+} , Fe^{2+} , and Zn^{2+} ; Fig. S12, Supplementary Material) in the presence of **4** in DMSO and the mass spectra were dominated by a singly charged peak of 744, which is likely assigned to the adduct $[\mathbf{4}(\text{SO}_4^{2-})(\text{H}^+)]^-$, further evidencing that strong SO_4^{2-} -involved hydrogen-bonding interactions exist.

In the case of Zn^{2+} in methanol, a Job plot analysis based on the emission data showed that the maximum intensity peaked at 448 nm and appeared at a mole fraction of 0.5, which corresponded to a 1 : 1 **4**-Zn complex, under the condition of an invariant total concentration in MeOH (Fig. 11). In accordance with this result, the HRMS analysis revealed a singly charged $[\mathbf{4} + \text{Zn} - 3\text{H}]^-$ complex, indicating that the deprotonation and coordination process occurred after addition of Zn^{2+} (Fig. S13,

Supplementary Material). In addition, the singly charged $[\mathbf{4} + \text{Cu} - 3\text{H}]^-$ complex was also observed by HRMS analysis (Fig. S14, Supplementary Material) when **4** interacted with Cu^{2+} in MeOH. The increase of fluorescent intensity and spectroscopic red-shift, which was attributed to SO_4^{2-} -involved hydrogen-bonding interactions in the early stage, was also not observed in MeOH when the Cu^{2+} and Zn^{2+} were added, instead of the rapid deprotonation and complexation. More interestingly, the emission intensity attributed to the metal Zn-complexes reached its maximum at a 3:1 ratio (Fig. 12) in the Job plot analysis of compound **1**, which is different from the 1 : 1 ratio of **4**. This type of conjugation-dependent difference in binding interaction was probably due to the decreased acidity, which would weaken the deprotonation capability of **1**. Compared with DMSO, the protic solvent MeOH can probably lead to a higher acidity of **4** to improve the Zn-metal complexation in the excited state, owing to the formation of contact and/or solvent-separated ion pairs.^[23] The results showed that the acidity of nitrilotribenzoic acid derivatives and the solvent environment are closely linked with the binding mode.

To further observe the interactions of **4** for other anions, aqueous solutions containing representative anions such as F^- , Cl^- , Br^- , I^- , ClO_4^- , NO_3^- , SO_3^{2-} , SO_4^{2-} , PO_4^{3-} , AcO^- , and S^{2-} (as their sodium salts) were also added respectively to a 3.5×10^{-5} M solution (DMSO) of **4** at room temperature (Fig. 13a, b). The original absorption peak at 329 nm was barely changed upon addition of Cl^- , Br^- , I^- , NO_3^- , and ClO_4^- . However, upon addition of the stronger basicity anions SO_3^{2-} , PO_4^{3-} , AcO^- , and S^{2-} , a noticeable enhancement of absorption intensity centred at ~ 331 nm was observed with a concomitant decrease at ~ 301 nm, demonstrating a strong hydrogen-bonding interaction between **4** and these anions. In addition, the emission peaks red-shifted from 474 to 486, 481, and 486 nm, with an obvious enhancement of intensity, after addition of F^- , PO_4^{3-} , and SO_4^{2-} . The emission intensity enhancement was probably related to a rigidifying effect which decreased the probability of a non-radiative decay upon addition of F^- , PO_4^{3-} , and SO_4^{2-} . Furthermore, the binding of Na^+ at the carbonyl group and the hydrogen-bonding interaction can increase the ICT character of the electronic transition, as evidenced by the red-shift of

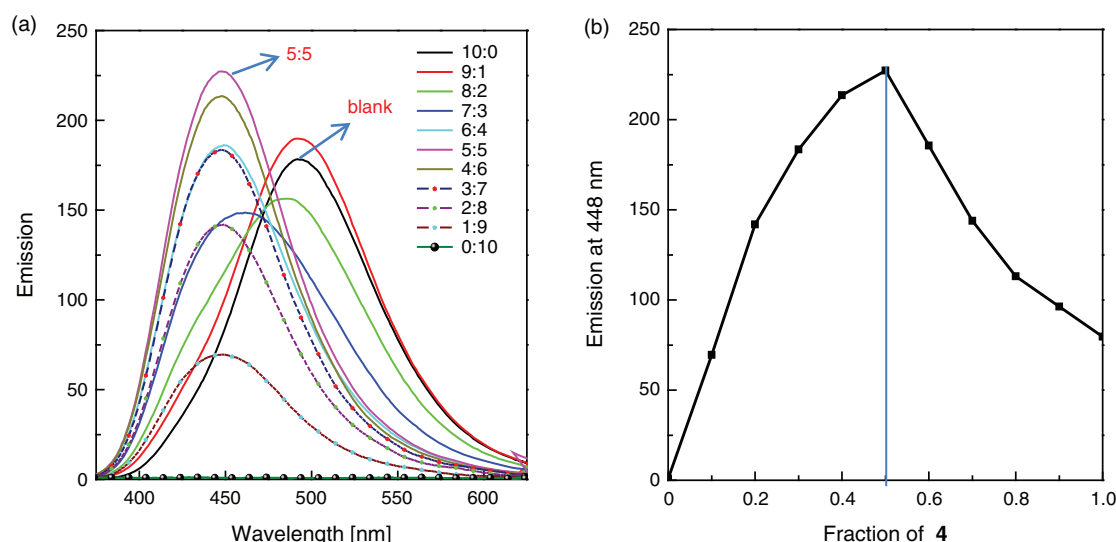


Fig. 11. Emission spectrum (a) of **4** in MeOH after addition of Zn²⁺ with different ratios of [salt]/[**4**], under the conditions of an invariant total concentration (5×10^{-5} M, λ_{ex} 325 nm). A Job plot analysis (b) between **4** and zinc sulfate.

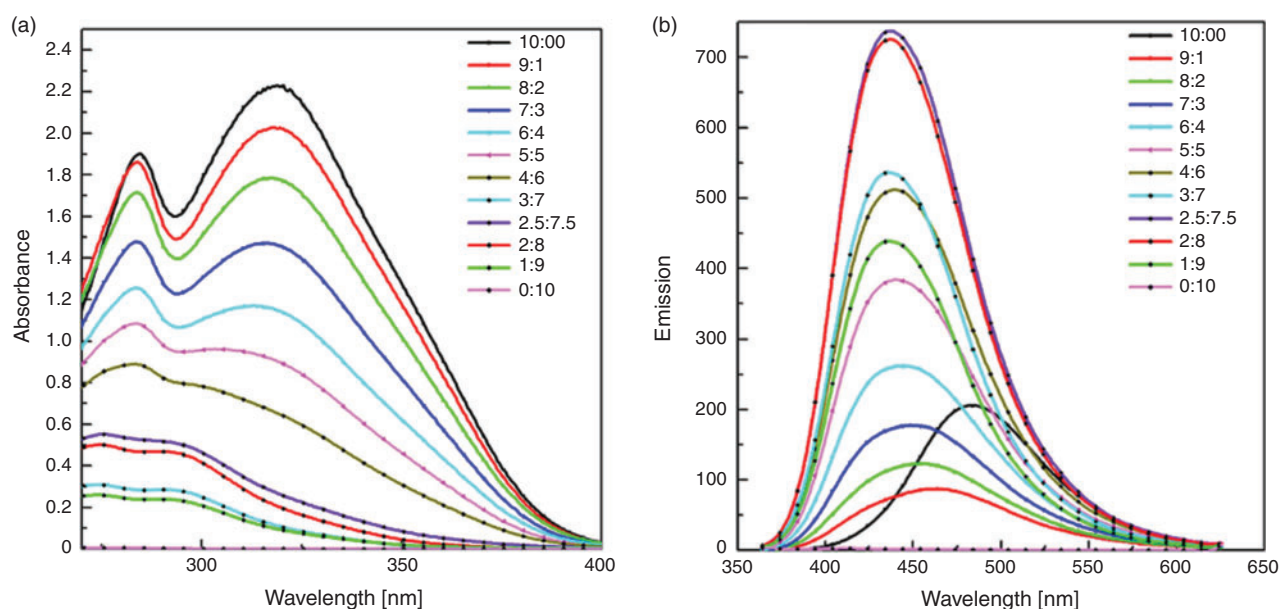


Fig. 12. Absorbance and emission spectrum of **1** in MeOH after addition of Zn²⁺ with different ratios of [1]/[salt], under the conditions of an invariant total concentration (3.5×10^{-4} M, λ_{ex} 325 nm).

absorption and emission after addition of F⁻ and SO₄²⁻ anions.^[24–27] Significantly, the emission peak at 474 nm was markedly blue-shifted respectively to 422 and 426 nm upon addition of the SO₃²⁻ and S²⁻ anions, which can be attributed to the strong interaction between carboxylic acids and anions. SO₃²⁻ and S²⁻ anions can possibly lead to strong hydrogen bonds in the ground state and the deprotonation of COOH and formation of carboxylate in the excited state, which probably weakened the ICT interaction from the HOMO mainly localised over the TPA unit to the LUMO localised in the carboxylate moieties, leading to the hypochromatic shift in emission.^[28] When anions were added to a 4×10^{-5} M protic solution (MeOH) of **4**, as shown in Fig. 13c, d, the absorption and emission peaks were negligibly changed upon addition of F⁻, Cl⁻, Br⁻, I⁻, NO₃⁻, ClO₄⁻, and SO₄²⁻. However, upon addition

of SO₃²⁻, PO₄³⁻, and S²⁻, the absorption peak at 326 nm was slightly blue-shifted to \sim 322 nm and the emission peak was obviously blue-shifted from 495 nm to 440, 436, and 441 nm, respectively. In addition, the close resemblance of the absorption and emission spectrum of **4** in the presence of SO₃²⁻, PO₄³⁻, and S²⁻ with those of the strong basicity anion OH⁻ in MeOH were consistent with the deprotonation of COOH units. However, the spectroscopic patterns for **4** with OH⁻ failed to have a close resemblance to the spectra in the presence of SO₃²⁻ and S²⁻ in DMSO (Fig. S15, Supplementary Material). The spectroscopic profile with NaOH experienced a slight blue-shift in absorption, whereas with SO₃²⁻ and S²⁻ a slight red-shift was observed, indicating the absence of the deprotonation by SO₃²⁻ and S²⁻ anions in the ground state,^[29] and anion-induced hydrogen-bonding interactions and deprotonation of the COOH

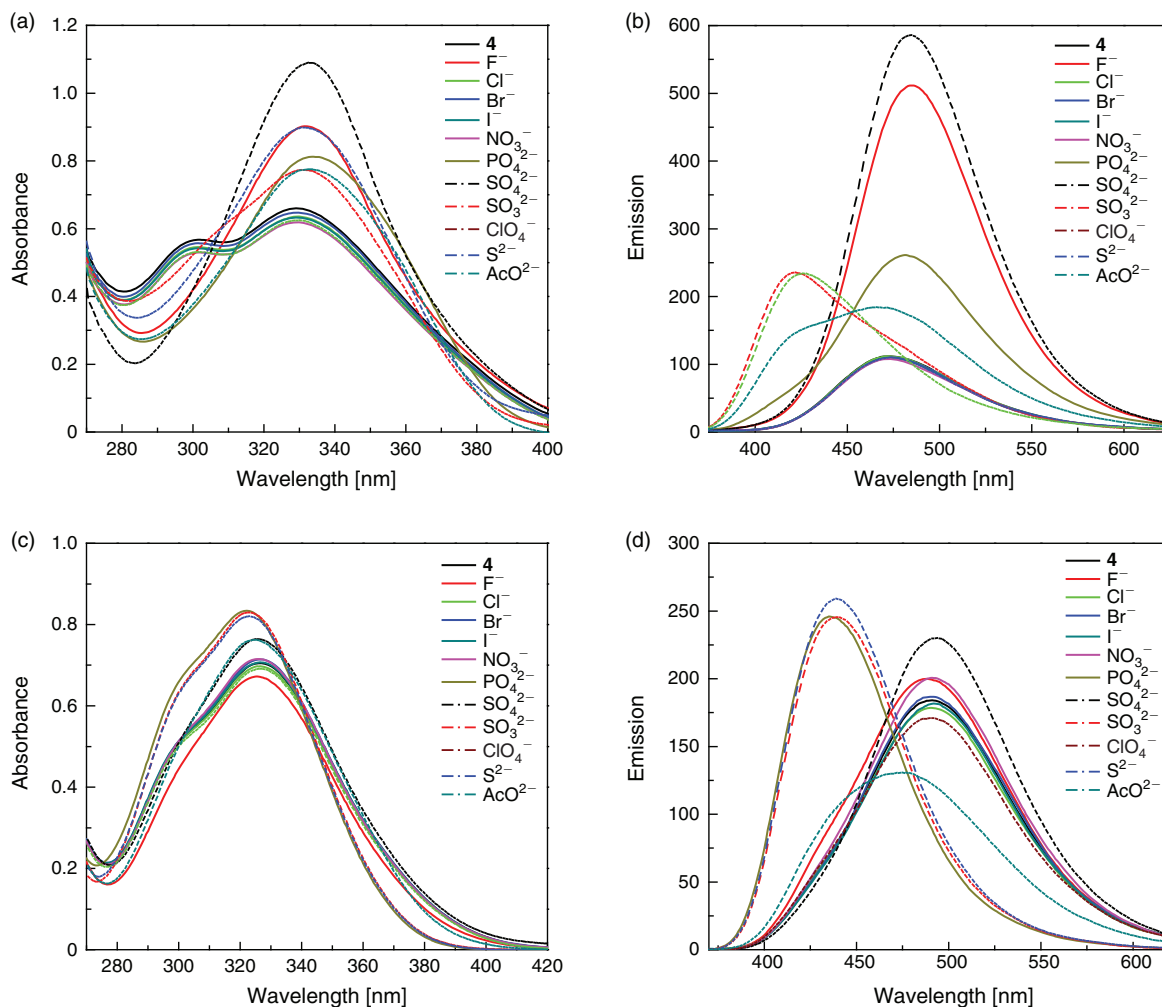


Fig. 13. Absorption and emission spectrum of **4** in DMSO (3.5×10^{-5} M, a and b, λ_{ex} 325 nm) and MeOH (4×10^{-5} M, c and d) after addition of anions with a 30 : 1 ratio of [anion] to [**4**].

protons of the receptors both existing in the excited state. The results showed that the basicity and geometrical configuration of anions and the solvent environment have an important effect on hydrogen-bonding interactions and deprotonation. Compound **4** can probably accommodate anions selectively through the formation of hydrogen bonds with the COOH moieties, which induces a change in the conformational conformation and rigidity. The above-mentioned different absorption and fluorescence outputs after addition of different anions in different solvent may be highly related to the acidity of **4**, the basicity of anions, the charge numbers, and the shape of the match between the hydrogen-bonding donor and acceptor groups.^[29]

In the past decades, several organic compounds containing pyrrole, imidazole, urea, or thiourea moieties that are capable of providing an acidic NH group have been widely reported to exhibit a strong affinity and selectivity towards certain anions.^[30] However, the application of 2,2',2''-nitrilotribenzoic acid derivatives to molecular sensing has not been reported. In addition, site selective binding to polyhistidine through transition metal ions (often Cu²⁺, Ni²⁺, and Zn²⁺) complexed by NTA attached to fluorophores, have been widely applied in molecular recognition and imaging in live cells under mild conditions.^[1] In our study, the 2,2',2''-nitrilotribenzoic acid ligand has a similarly tetradentate NO₃ donor to form complexes

and can be potentially applied as an alternative to the NTA ligand. The readily modifiable C₃ symmetry can be utilised to build a series of water-soluble conjugated fluorescent sensors by molecular extension in the 4,4',4''' positions. The efforts in developing 2,2',2''-nitrilotribenzoic acid derivatives and their metal complexes for anion sensing are in progress and will be reported in a forthcoming paper.

Conclusions

In summary, a C₃-symmetrical 4,4',4'''-nitrilotris(2'-methyl-[1,1'-biphenyl]-3-carboxylic acid) (**4**) has been synthesized for ion recognition. Nitrilotribenzoic acid, comprised of a triphenylamine backbone and three carboxylic units in the 2,2',2''-positions, can pre-organise to form a cavity for ion capture. The observed sensing process of sulfate salts associated with the SO₄²⁻-involved hydrogen-bonding interactions, deprotonation, and concomitant complexation can also be clearly monitored by titration methods using UV-vis, fluorescence, and NMR spectroscopy in solution. The results show that **4** can bear high selectivity and sensitivity for Zn²⁺ ions in the presence of other competitive metal ions with a 1:1 binding stoichiometry. Anion-induced hydrogen-bonding interactions and deprotonation of the COOH groups in the excited state also endows **4** versatile spectroscopic properties. The 2,2',2''-nitrilotribenzoic

acid can be utilised as a potential scaffold to build a series of conjugated fluorescent sensors by its chelation effect owing to the rigid cavity pre-organised by the triphenylamine moiety and the carboxylic groups and conjugation extension in the 4,4',4'' positions.

Supplementary Material

The ^1H -NMR and ^{13}C -NMR spectra, the ESI spectrum, and absorption and emission spectra of **4** after addition of salts are available on the Journal's website.

Conflicts of Interest

The authors declare no conflicts of interest.

Acknowledgements

This work is financially supported by the National Natural Science Foundation of China (21772014 and 21372029).

References

- [1] M. Kruppa, B. König, *Chem. Rev.* **2006**, *106*, 3520. doi:10.1021/CR010206Y
- [2] Y. Mikata, K. Kawata, S. Iwatsuki, H. Konno, *Inorg. Chem.* **2012**, *51*, 1859. doi:10.1021/IC202159V
- [3] J. Klenc, M. Lipowska, P. L. Abhayawardhana, A. T. Taylor, L. G. Marzilli, *Inorg. Chem.* **2015**, *54*, 6281. doi:10.1021/ACS.INORG.CHEM.5B00584
- [4] A. S. Jullien, C. Gateau, I. Kieffer, D. Testemale, P. Delangle, *Inorg. Chem.* **2013**, *52*, 9954. doi:10.1021/IC401206U
- [5] V. Roullier, S. Clarke, C. J. You, F. Pinaud, G. Gouzer, D. Schaible, V. Marchi-Artzner, J. Pichler, M. Dahan, *Nano Lett.* **2009**, *9*, 1228. doi:10.1021/NL9001298
- [6] K. Peneva, G. Mihov, A. Herrmann, N. Zarrabi, M. Börsch, T. M. Duncan, K. Müllen, *J. Am. Chem. Soc.* **2008**, *130*, 5398. doi:10.1021/JA711322G
- [7] K. L. Cheng, *Anal. Chem.* **1958**, *30*, 1035. doi:10.1021/AC60138A007
- [8] M. Gabričević, A. L. Crumbliss, *Inorg. Chem.* **2003**, *42*, 4098. doi:10.1021/IC026281O
- [9] X. Q. Lu, J. J. Jiang, C. L. Chen, B. S. Kang, C. Y. Su, *Inorg. Chem.* **2005**, *44*, 4515. doi:10.1021/IC050125A
- [10] S. J. Jeon, S. Y. Kwak, D. B. Yim, J. M. Ju, J. H. Kim, *J. Am. Chem. Soc.* **2014**, *136*, 10842. doi:10.1021/JA504276Z
- [11] A. J. Zuccherro, J. N. Wilson, U. H. F. Bunz, *J. Am. Chem. Soc.* **2006**, *128*, 11872. doi:10.1021/JA061112E
- [12] W. F. Li, H. C. Ma, Z. Q. Lei, *RSC Adv.* **2014**, *4*, 39351. doi:10.1039/C4RA05843G
- [13] Y. D. Hang, J. Wang, T. Jiang, N. N. Lu, J. L. Hua, *Anal. Chem.* **2016**, *88*, 1696. doi:10.1021/ACS.ANALCHEM.5B03715
- [14] K. Ghosh, G. Masanta, R. Fröhlich, I. D. Petsalakis, G. Theodorakopoulos, *J. Phys. Chem. B* **2009**, *113*, 7800. doi:10.1021/JP901151W
- [15] J. J. Yao, Y. Y. Fu, W. Xu, T. C. Fan, Y. X. Gao, Q. Q. He, D. F. Zhu, H. M. Cao, J. G. Cheng, *Anal. Chem.* **2016**, *88*, 2497. doi:10.1021/ACS.ANALCHEM.5B04777
- [16] A. Chowdhury, P. S. Mukherjee, *J. Org. Chem.* **2015**, *80*, 4064. doi:10.1021/ACS.JOC.5B00348
- [17] H. C. Ma, Z. W. Zhang, Y. Y. Jin, L. J. Zha, C. X. Qi, H. Y. Cao, Z. M. Yang, Z. W. Yang, Z. Q. Lei, *RSC Adv.* **2015**, *5*, 87157. doi:10.1039/C5RA12154J
- [18] Z. Peng, X. H. Yi, Z. X. Liu, J. Shang, D. Y. Wang, *ACS Appl. Mater. Interfaces* **2016**, *8*, 14578. doi:10.1021/ACSAMI.6B03418
- [19] S. Wörl, D. Hellwinkel, H. Pritzkowa, R. Krämer, *Chem. Commun.* **2003**, 2506. doi:10.1039/B307277K
- [20] S. Wörl, I. O. Fritsky, D. Hellwinkel, H. Pritzkow, R. Krämer, *Eur. J. Inorg. Chem.* **2005**, 759. doi:10.1002/EJIC.200400698
- [21] M. J. Yuan, Y. L. Li, J. B. Li, C. H. Li, X. F. Liu, J. Lv, J. L. Xu, H. B. Liu, S. Wang, D. B. Zhu, *Org. Lett.* **2007**, *9*, 2313. doi:10.1021/OL0706399
- [22] S. Goswami, D. Sen, N. K. Das, *Org. Lett.* **2010**, *12*, 856. doi:10.1021/OL9029066
- [23] S. Mandal, S. Ghosh, C. Banerjee, J. Kuchlyan, N. Sarkar, *J. Phys. Chem. B* **2013**, *117*, 12212. doi:10.1021/JP406853R
- [24] Y. Cui, H. J. Mo, J. C. Chen, Y. L. Niu, Y. R. Zhong, K. C. Zheng, B. H. Ye, *Inorg. Chem.* **2007**, *46*, 6427. doi:10.1021/IC7004562
- [25] P. Ashokkumar, V. T. Ramakrishnan, P. Ramamurthy, *J. Phys. Chem. B* **2011**, *115*, 84. doi:10.1021/JP107717Z
- [26] P. Ashokkumar, V. T. Ramakrishnan, P. Ramamurthy, *J. Phys. Chem. A* **2011**, *115*, 14292. doi:10.1021/JP209061F
- [27] R. Wagner, W. Wan, M. Biyikal, E. Benito-Peña, M. Moreno-Bondi, I. Lazraq, K. Rurack, B. Sellergren, *J. Org. Chem.* **2013**, *78*, 1377. doi:10.1021/JO3019522
- [28] W. C. Lin, S. K. Fang, J. W. Hu, H. Y. Tsai, K. Y. Chen, *Anal. Chem.* **2014**, *86*, 4648. doi:10.1021/AC501024D
- [29] F. Zapata, A. Caballero, A. Espinosa, A. Tárraga, P. Molina, *J. Org. Chem.* **2008**, *73*, 4034. doi:10.1021/JO800296C
- [30] M. E. Moragues, R. Martínez-Mañez, F. Sancenón, *Chem. Soc. Rev.* **2011**, *40*, 2593. doi:10.1039/C0CS00015A